

Synthesis, X-ray diffraction and dielectric studies of the ceramic samples $(1-x)\text{BaTiO}_3 \cdot x\text{PbFe}_{2/3}\text{W}_{1/3}\text{O}_3$ ($0 \leq x \leq 1$) system

D. Yu. Fedulov , K. E. Kamentsev , A. A. Bush * and V. I. Kozlov 

Research Institute of Solid-State Electronics Materials
MIREA - Russian Technological University
Vernadskogo Avenue 78, 119454, Moscow, Russia
*aabush@yandex.ru

Received 13 December 2023; Revised 19 January 2024; Accepted 20 February 2024; Published 16 March 2024

Ceramic samples of the $(1-x)\text{BaTiO}_3 \cdot x\text{PbFe}_{2/3}\text{W}_{1/3}\text{O}_3$, $0 \leq x \leq 1$ ($(1-x)\text{BT} \cdot x\text{PFW}$) system were synthesized by solid-state reactions method. The samples were characterized by X-ray diffraction (XRD) and dielectric studies, as well as by the measurements of the thermally stimulated depolarization currents (TSDC). It was found that the predominant phase in the samples is presented by the $(\text{Ba}_{1-x}\text{Pb}_x)(\text{Ti}_{1-x}\text{Fe}_{2x/3}\text{W}_{x/3})\text{O}_3$ solid solutions with a perovskite structure, herewith the samples with $0 \leq x < 0.25$ are practically single-phase, and with $0.25 \leq x < 1$ contain the impurity phase BaWO_4 (up to 15 mass.% at $x = 0.60\text{--}0.90$). Information has been obtained about the changes in the structural and dielectric characteristics of the solid solutions with the change of their composition. It is established that the solid solutions crystal lattice symmetry at 296 K changes from tetragonal at $x \leq 0.04$ to cubic at $x \geq 0.05$. An increase in the PFW content in solid solutions causes a gradual change in their properties from ferroelectric at $0 \leq x < 0.10$ to relaxor ferroelectric at $0.10 \leq x \leq 0.25$, and then to properties similar to those of the dipole glass with weak or zero correlation between dipoles at $0.25 < x \leq 0.90$. The addition of BT to PFW leads to rather quick degradation of the relaxor ferroelectric properties of PFW in the region $x = 0.9\text{--}1.0$.

Keywords: $\text{BaTiO}_3\text{--PbFe}_{2/3}\text{W}_{1/3}\text{O}_3$ system; ceramics; solid solutions; X-ray diffraction phase analysis; dielectric properties; ferroelectrics; relaxor ferroelectrics.

1. Introduction

Solid solutions with a perovskite crystal structure based on ferroelectric barium titanate BaTiO_3 possess interesting properties from a scientific and applied point of view. Therefore, they have been intensively studied over the past few decades.^{1–5} As a result, a variety of these kinds of solid solutions have been obtained and studied, and many of them have found applications, e.g., as condenser, posistor, piezoelectric materials, etc. Nevertheless, it should be noted that the solid solutions of a potentially promising system $(1-x)\text{BaTiO}_3 \cdot x\text{PbFe}_{2/3}\text{W}_{1/3}\text{O}_3$ (BT–PFW) remain very poorly studied. Only one work has been found by us on this system,⁶ which presents the results of preliminary studies of the dielectric and magnetic properties, as well as of their Mössbauer spectra on the ceramic samples with $0.70 \leq x \leq 1$. In this work, the temperature dependences of the real part of the permittivity $\varepsilon_1(T)$ were studied at a fixed frequency $f = 100$ kHz. We show that the conclusion made in Ref. 6 about the relationship of the maxima observed in the dependences $\varepsilon_1(T)$ with ferroelectric phase transitions needs to be clarified, since the reason appearance of this maxima can be connected with the dielectric relaxation occurring in the samples.

Barium titanate with a perovskite structure exhibits bright ferroelectric properties with a Curie point equal to

$T_C = 403$ K, where the symmetry of crystals changes from cubic (C) to tetragonal (T). In barium titanate, below T_C , two-phase transitions of the first order were observed, from tetragonal to orthorhombic (O), and from orthorhombic to rhombohedral (R) phase, at $T_{T/O} \approx 273$ K and $T_{O/R} \approx 183$ K, respectively.^{1–5}

Unlike the tetragonal ferroelectric phase BaTiO_3 , lead ferro tungstate PFW has cubic symmetry at all temperatures and does not exhibit ferroelectric properties, showing typical response for relaxor ferroelectrics (RFEs).^{2,7–12} In the temperature dependence of permittivity, $\varepsilon_1(T)$, a blurred relaxation maximum is observed at $T_m \approx 190$ K with a high value of dielectric permittivity, $\varepsilon_{1m} \approx 5000$, the behavior typical for RFEs. The position T_m of this maximum shifts with frequency growth toward high temperatures, obeying the Vogel–Fulcher law

$$f = (1/2\pi\tau_0) \exp[E_a/k_B(T_m - T_{VF})], \quad (1)$$

where k_B is the Boltzmann constant, τ_0 , E_a and T_{VF} are the fitting parameters.¹¹ For classical relaxor ferroelectric of the $\text{PbMg}_{1/3}\text{Nb}_{2/3}\text{O}_3$ type they are considered as relaxation time at high temperature ($T \rightarrow \infty$), the activation energy for polarization fluctuations of a separate polar nanoregion (PNR), the Vogel–Fulcher freezing temperature. It is believed that

at temperatures below T_{VF} , the dynamics of PNRs freeze (they become static) and the system passes into a nonergodic relaxor glassy state with the directions of the dipole moments of individual PNRs randomly fixed in different directions.¹¹

The noted differences between BT and PFW indicate that changes in the composition of the $(1-x)BT \cdot xPFW$ solid solutions will cause changes in the symmetry of their crystal lattice and the realization of various dielectric states. Additional interest in the study of the PFW is caused by the coexistence of the relaxor ferroelectric and antiferromagnetic properties.^{2,7–12} Due to the relatively high temperature of the magnetic phase transition ($T_N = 363$ K), PFW is considered a promising component that can be used to create new magnetolectric compositions.

In the family of perovskite-like phases $A[B1]_{1-m}[B2]_mO_3$, $m = 1/2, 1/3$, the PFW phase has the lowest sintering temperature ($< 900^\circ\text{C}$). Therefore, PFW is used as an additive to other relaxor compositions to reduce their sintering temperature below 1000°C .^{2,12–14} Such a reduction is important for dielectric materials used in the development of multilayered ceramic capacitors since the high sintering temperature of $BaTiO_3$ ($> 1300^\circ\text{C}$) makes it necessary to use expensive metal, Pd, as internal electrodes. Lowering the sintering temperature makes it possible to sinter multilayer ceramic capacitors together with relatively inexpensive interlayer electrodes with a low melting point, such as Ag/Pd alloys.

In connection with the above, the purpose of this work was to obtain ceramic samples of the $(1-x)BT \cdot xPFW$, $0 \leq x \leq 1$ system and to study its structural and dielectric properties.

2. Experimental Procedure

2.1. Synthesis of ceramics

The samples were synthesized in an air atmosphere by solid phase reactions method using conventional ceramic technology. The oxides of the PbO (brand “G-2” with at least 98.7% of the base substance), TiO_2 (extra pure grade, $\geq 99.9\%$), Fe_2O_3 (analytical grade, $\geq 99\%$), WO_3 (high-purity grade, $> 99.9\%$) and barium carbonate $BaCO_3$ (analytical grade, $> 99\%$) were used as starting materials. The compositions of the synthesized and studied samples corresponded to the formula $(1-x)BaTiO_3 \cdot xPbFe_{2/3}W_{1/3}O_3$ (BT–PFW) with $x = 0–1$. The charge for ceramic synthesis was prepared by homogenizing mixtures of the above components by mixing them in a porcelain mortar in an air environment.

The annealing of the homogenized mixtures was carried out in a furnace SNOL 12/16 (Technoterm, Russia) at a temperature of $800–1230^\circ\text{C}$ for 4 h with several intermediate cooldowns and grindings of the annealed products. The annealing temperature with the growth of x was gradually reduced from 1230°C for $x = 0$ to 800°C for $x = 1$.

The annealing products were crushed and formed into cylindrical disks with a diameter of $D \approx 10$ mm and a

thickness of 1–3 mm at a pressure of $p \approx 60$ MPa. The obtained disks were sintered for 2–4 h at temperatures about 100°C above the annealing temperatures. As a result, the ceramic samples were obtained with densities equal to 80–95% of the theoretical density. To study the electro-physical properties of the obtained samples, electrodes were deposited on their base planes by burning an Ag-containing paste at $T \approx 850^\circ\text{C}$.

2.2. X-ray diffraction studies

The phase composition of the synthesized ceramic samples was determined by X-ray diffraction (XRD) using an upgraded X-ray diffractometer DRON-4 (Bourestnik, Russia) with filtered cobalt radiation. Ge powdered crystals were used as an internal standard. The ICDD database was used for phase identification.¹⁵

2.3. Dielectric studies

Measurements of the real part (ε_1) of the complex dielectric permittivity ($\varepsilon^* = \varepsilon_1 - i\varepsilon_2$) and the loss tangent $\tan\delta$ of the synthesized samples were carried out by using the immittance meter E7-30 (MNIPI, Belarus) in the temperature range $T = 80–700$ K and in the frequency interval $f = 25$ Hz–1 MHz, with the amplitude of the probing electric signal equal to 1 V. The imaginary part ε_2 of the complex permittivity was calculated using the expression $\varepsilon_2 = \varepsilon_1 \cdot \tan\delta$.

2.4. Measurements of thermally stimulated depolarization currents

Measurements of thermally stimulated depolarization currents (TSDC) of the samples were performed in the short-circuit mode with a universal voltmeter-electrometer V7-30 when samples were heated at a rate of 0.2–0.4 K/s in the temperature range of 80–420 K (10–300 K in some cases). The polarization of the samples was carried out by applying a permanent electric field with a strength of 1.5–2.5 kV/cm to them during their cooling from temperatures exceeding the temperature of ferroelectric or relaxor maximum observed on the dependences $\varepsilon_1(T)$.

3. Results and Discussion

3.1. Results of the X-ray diffraction studies

XRD shows that the predominant phase in the samples is the $(Ba_{1-x}Pb_x)(Ti_{1-x}Fe_{2x/3}W_{x/3})O_3$ solid solutions with a perovskite structure (Fig. 1(a)). The samples with $0 \leq x < 0.25$ were practically single-phase, and the samples with $0.25 \leq x < 1$ contained an impurity of the tetragonal phase with the parameters $a = 5.620$ Å, $c = 12.73$ Å corresponding to $BaWO_4$.¹⁵ The maximum content of this impurity phase reached 15 wt. % at $x = 0.60–0.90$. On the XRD patterns of the samples with $0 \leq x < 0.05$, the splitting of reflexes characteristic of tetragonal phases was observed. At $x \geq 0.05$, there is no splitting of reflections (Fig. 1(b)).

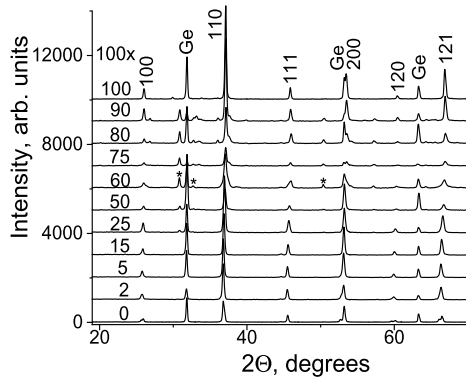


Fig. 1(a). XRD patterns of the $(1-x)\text{BT} \cdot x\text{PFW}$ samples with additives of Ge crystal powder as an internal standard: Miller indices are indicated above the solid solutions peaks, peaks of the impurity phase BaWO_4 are marked with an asterisk (CoK α -radiation).

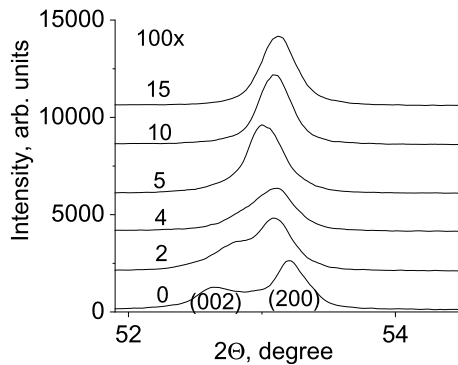


Fig. 1(b). Fragments of XRD patterns of the samples without additives of Ge, illustrating the splitting of the (002)–(200) reflections at $x < 0.05$.

Concentration dependences of the unit cell parameters of the solid solutions and their crystal lattice symmetry at 296 K are shown in Fig. 2. The addition of PFW to barium titanate gradually reduces the degree of its tetragonality c/a ; for $x = 0.05$ it becomes equal to 1, and the crystal lattice of the solid solutions in the region $x = 0.05$ –1 acquires cubic symmetry.

An increase in the PFW content in the solid solutions leads to a decrease of the reduced unit cell parameter $a_p = (a^2c)^{1/3}$ in the concentration range $x = 0$ –0.80. This decrease in a_p is replaced by an increase in the region $x = 0.80$ –1. Such feature of the $a_p(x)$ dependence is explained by the fact that the predominant effect on the a_p of the solid solutions $(\text{Ba}_{1-x}\text{Pb}_x)(\text{Ti}_{1-x}\text{Fe}_{2x/3}\text{W}_{x/3})\text{O}_3$ in these concentration ranges is a decrease in the average cationic size at the A position of the perovskite structure ($r(\text{Ba}^{2+}) = 1.61 \text{ \AA}$, $r(\text{Pb}^{2+}) = 1.49 \text{ \AA}$),¹⁶ and an increase in the average cation size at the B position of the perovskite structure ($r(\text{Ti}^{4+}) = 0.605 \text{ \AA}$, $r(\text{Fe}_{2/3}^{3+}\text{W}_{1/3}^{6+}) = 0.630 \text{ \AA}$), respectively.¹⁶

3.2. Results of the dielectric measurements

The results of the dielectric measurements are presented in Figs. 3, 4, A.1 and A.2 in the form of the temperature-frequency

dependencies of $\varepsilon_1(T, f)$, $\varepsilon_2(T, f)$ and $\tan\delta(T, f)$. Figure 2 presents the concentration dependencies of the temperature at which the maximum is observed in the dependence $\varepsilon_1(T)$, of the magnitude ε_1 at the maximum (ε_{1m}) and at room temperature ($\varepsilon_{1\text{RT}}$), of the peak width (ΔT_m) at half height of the maximum. The dependences $\varepsilon_1(T, f)$ and $\tan\delta(T, f)$ of the BT samples display three pronounced maxima corresponding to the phase transitions occurring in the BT and leading to successive changes of its symmetry from cubic to tetragonal (at the Curie point $T_C = 408 \text{ K}$), from tetragonal to orthorhombic (at $T_{\text{T/O}} = 288 \text{ K}$) and from orthorhombic to rhombohedral (at $T_{\text{O/R}} = 195 \text{ K}$) (Fig. A.1), by the literature data for BT.^{1–5}

Samples with $x = 0$ –0.04 exhibit ferroelectric properties similar to those of BT with three phase transitions at T_C , $T_{\text{T/O}}$ and $T_{\text{O/R}}$ (Figs. 3 and A.1). Addition of the PFW component to BT causes a decrease in T_C and $T_{\text{T/O}}$ and an increase in $T_{\text{O/R}}$, (Figs. 2, 3 and A.1). As a result, the temperatures of these phase transitions converge. At $x \approx 0.08$, the three-phase transition temperatures merge, and at $x > 0.08$, the solid solutions exhibit only one phase transition, whose temperature decreases to 245 K as the PFW content grows up to $x = 0.09$. In the concentration range $0.05 \leq x < 0.10$, there is a significant broadening of the maximum in $\varepsilon_1(T)$ around T_C , which is characteristic of ferroelectrics with a diffuse phase transition (FE DPT).

Shift toward high temperatures of the maxima positions seen in the temperature dependences of the real (at T_m) and imaginary (at T_{mi}) parts of the dielectric permittivity with increasing frequency for samples with $x \geq 0.10$ (Figs. 3, 4 and A.1) indicates relaxor character of these maxima.

In the concentration region $0.10 \leq x \leq 0.25$, the solid solutions exhibit dielectric properties that are characteristic of the RFEs of the PMN type. There is a broad maximum in dependences $\varepsilon_1(T, f)$ and $\varepsilon_2(T, f)$ which shows a pronounced frequency dispersion (Figs. 3, 4 and A.1); as in other relaxors, the temperatures of these maxima T_m and T_{mi} shift to high temperatures during frequency f growth, following the Vogel–Fulcher law $f = f_0 \exp[E_a/k_B(T_{\text{mi}(i)} - T_{\text{VF}})]$ (Fig. 4).¹¹ The values of the fitting parameters f_0 , E_a , T_{VF} were determined by processing the $T_{\text{mi}}(f)$ dependencies with the Vogel–Fulcher formula; found parameters' values (see, Fig. 4) correspond well to those known for RFEs. We thus conclude that the studied solid solutions in the range $0.10 \leq x \leq 0.25$ belong to the class of RFEs.

A further increase in the PFW content in the samples in the range $0.25 < x \lesssim 0.90$ leads to a significant decrease and blurring of the maximum observed on the $\varepsilon_1(T)$ dependence in the temperature range 100–200 K, herewith its dependence $\varepsilon_1(T, f)$ ceases to exhibit the frequency dispersion characteristic of RFEs. At $x = 0.75$ and 0.80, these maxima practically do not manifest itself (Fig. A.1).

The addition of the BT component to the PFW phase in the region $x = 0.9$ –1 leads to a rather sharp degradation of its ferroelectric relaxation properties which manifests itself in

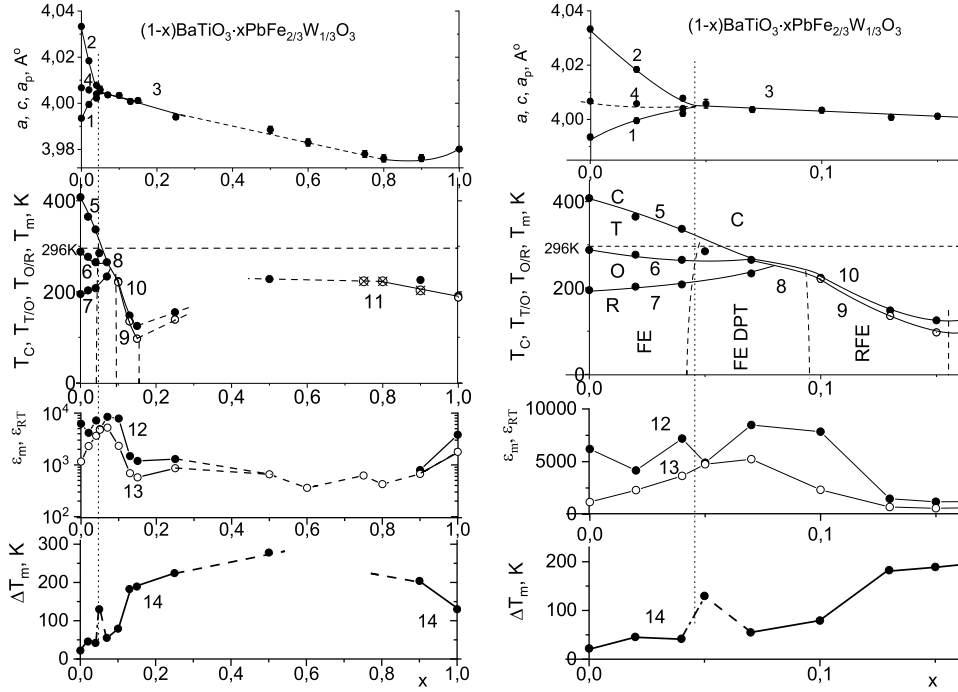


Fig. 2. Concentration dependences of the characteristics of the $(1-x)\text{BT} \cdot x\text{PFW}$ solid solutions: parameters of the tetragonal a (1) and c (2), cubic a (3) and reduced $a_p = (a^2c)^{1/3}$ (4) unit cell; temperatures of the phase transitions T_C (5, 8), $T_{T/O}$ (6), $T_{O/R}$ (7) and relaxor maximums T_m (9–11, 11 – data from Ref. 6); dielectric permittivity measured at $T = T_{c(m)}$ (ϵ_{1m} – 12) and at room temperature (ϵ_{1RT} – 13); width ΔT_m at half height of the maximum observed in the dependence $\epsilon_1(T)$ (14) (9 at $f = 120\text{Hz}$, 10–14 at $f = 100\text{kHz}$, C, T, O, R denotes cubic, tetragonal, orthorhombic, rhombohedral symmetries, respectively). (On the right graph, the scale is stretched along the x -axis.)

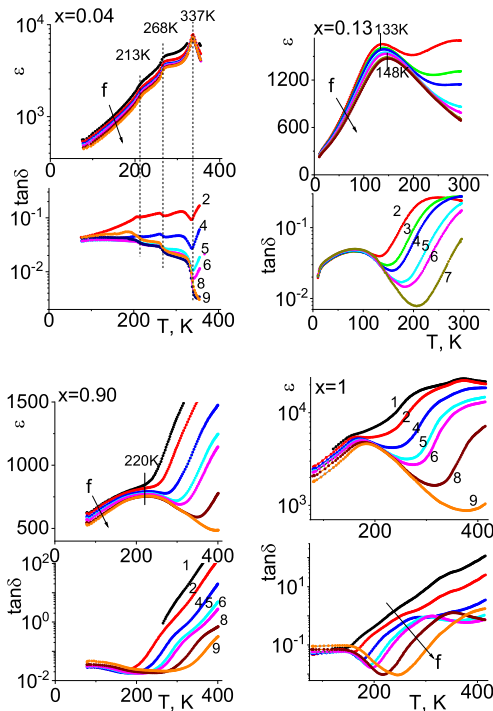


Fig. 3. Dependences $\epsilon_1(T)$ and $\tan\delta(T)$ (measured at f , kHz: 0.025 – curves 1, 0.120 – 2, 1 – 4, 5 – 5, 10 – 6, 100 – 8, 1000 – 9) for the $(1-x)\text{BT} \cdot x\text{PFW}$ samples with $x = 0.04, 0.13, 0.90$ and 1.

the disappearance of the dependence of T_m on f and a significant decrease in the value of ϵ_{1m} (Fig. A.1, $x = 0.90$).

Thus, an increase in the PFW content in $(1-x)\text{BT} \cdot x\text{PFW}$ solid solutions causes a change in their dielectric properties from FE in the region $0 \leq x < 0.10$, to RFE in the region $0.10 \leq x \leq 0.25$, then to nonferroelectric and nonrelaxor ferroelectric in the region $0.25 < x \lesssim 0.90$ and then again to RFE in the region $0.90 \lesssim x \leq 1$. Such behavior can be explained, apparently, by a change in the ferroelectrically active sublattice of $(1-x)\text{BT} \cdot x\text{PFW}$ solid solutions from Ti to Pb with an increase in them PFW content.^{2,10,11} An increase in the PFW content leads to a decrease in the content of ferroelectrically active Ti cations and, accordingly, to a weakening of correlations between the dipole moments of TiO_6 octahedra, it prevents the formation of PNRs. Similarly, an increase in the BT content in the region of $0.90 \lesssim x \leq 1$ causes a decrease in the content of ferroelectrically active Pb cations, followed by a loss of RFE properties. Due to the presence in the structure of solid solutions with $0.25 < x \lesssim 0.90$ dipole structural units arising from displacements of Ti^{4+} and/or Pb^{2+} cations from their central positions,^{4,10,11} it can be assumed that solid solutions of these compositions can be classified as dipole glasses with weak or no correlations between dipoles even at low temperatures.

The high ϵ_{1m} value measured at the maximum in the dielectric constant of BT is preserved in the solid solutions

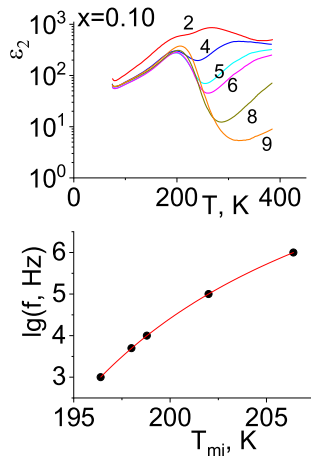


Fig. 4. Dependence of $\lg f$ on T_{mi} for ceramics $(1-x)\text{BT} \cdot x\text{PFW}$ with $x = 0.10$ (f , kHz: 0.12 (curve 2), 1 (4), 5 (5), 10 (6), 100 (8) and 1000 (9)). The line shows the results of the fitting according to the Vogel–Fulcher law with $f_0 = 1.5 \cdot 10^{11}$ Hz, $E_a = 0.028(8)$ eV, $T_{VF} = 179(1)$ K, experimental data are shown by circles dots.

with $x = 0-0.10$ ($\varepsilon_{1m} \approx 5000-8000$). Further increase of the PFW content in the samples caused a rather sharp decrease in maximum magnitude to 1500 at $x = 0.13$ (Figs. 2, 3 and A.1). Transition from the concentration region of FE compositions ($x < 0.10$) to the region of RFE compositions ($0.10 \leq x \leq 0.25$) is accompanied by a significant broadening of the ε_1 peak on the dependence $\varepsilon_1(T)$ at T_C or T_m (Figs. 3, A.1 and A.2). The presence of a sharp local maximum ΔT_m on the $\Delta T_m(x)$ dependence at $x = 0.05$ (Fig. 2) is obviously caused by the fact that for $x = 0.05$, the three peaks ε_1 at T_C , $T_{T/O}$, $T_{O/R}$ approached each other so closely that it is impossible to distinguish from the general broad peak ε_1 the contribution from the peak at T_C .

Note that the presence, at high temperatures ($T > 250$ K) on the $\varepsilon_1(T)$ and $\tan\delta(T)$ dependences in some compositions, of the relaxation maxima that show temperature-activated behavior with an activation energy $E_a \approx 0.40$ eV (Figs. 3 and A.1), is probably caused by the mobile oxygen vacancies, the presence of which is inherent in samples of lead-containing oxides.^{12,17}

3.3. Results of the thermally stimulated depolarization currents measurements

Three pronounced maxima are observed in the dependences of the TSDC(T) of ferroelectric samples with $x = 0-0.04$ (Figs. 3 and A.1), the position of which corresponds to the temperatures of phase transitions taking place at T_C , $T_{T/O}$ and $T_{O/R}$. These maxima are obviously caused by C/T, T/O, O/R phase transitions, while the currents in the samples are pyroelectric in nature.

Contrary to the FE compositions, for the RFE compositions ($0.10 \leq x \leq 0.25$, $0.90 \lesssim x \leq 1$) the temperature of the current maximum is much lower than the temperature of the dielectric

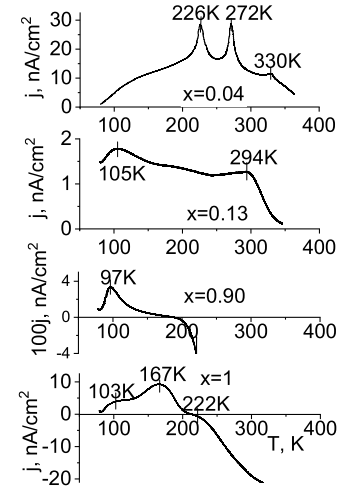


Fig. 5. Temperature dependences of TSDC for the samples with $x = 0.04$, 0.13, 0.90 and 1.

maximum (Figs. 5 and A.1), the difference between the two can reach 50–150 K. The proximity of the low-temperature maximum position of TSDC to the Vogel–Fulcher temperature found in the RFE compositions suggests that the occurrence of this maximum can be caused by the depolarization of the polar state of the sample, which arises due to some ordering of the electric dipoles when the sample was cooled in the polarizing electric field below the freezing temperature T_{VF} . Similar maxima of the TSDC(T) dependences were observed for the other RFEs, e.g., $(1-x)\text{PbMg}_{1/3}\text{Nb}_{2/3}\text{O}_3-x\text{PbSc}_{1/2}\text{Nb}_{1/2}\text{O}_3$, $x = 0.05$, 0.10, $\text{BaZr}_x\text{Ti}_{1-x}\text{O}_3$, $x = 0.35$, $\text{Pb}(\text{Fe}_{1-x}\text{Co}_x)_{2/3}\text{W}_{1/3}\text{O}_3$, $0 \leq x < 0.20$.^{12,18,19}

4. Conclusions





- (1) Using the solid phase reaction method, the ceramic samples of the $(1-x)\text{BaTiO}_3 \cdot x\text{PbFe}_{2/3}\text{W}_{1/3}\text{O}_3$, $x = 0-1$ system were synthesized. The performed XRD phase analysis showed that the predominant phase in the samples is $(\text{Ba}_{1-x}\text{Pb}_x)(\text{Ti}_{1-x}\text{Fe}_{2x/3}\text{W}_{x/3})\text{O}_3$ solid solutions with a perovskite structure, herewith samples with $x = 0-0.25$ are practically single-phase, and samples with $x \geq 0.25$ contain up to 15 mass.% of the impurity BaWO_4 phase.
- (2) The increase of the PFW content in the samples causes an increase of the solid solutions crystal lattice symmetry at room temperature from tetragonal at $x \leq 0.04$ to cubic at $x \geq 0.05$.
- (3) In the temperature range 100–570 K and in the frequency interval 25 Hz–1 MHz, the temperature-frequency dependences of the permittivity $\varepsilon_1(T, f)$ and the loss tangent $\tan\delta(T, f)$ of the obtained samples were studied. The TSDC in the samples was studied in the range of 100–420 K. It is established that the growth of the PFW content in the $(1-x)\text{BT} \cdot x\text{PFW}$ solid solutions causes a

gradual change in their dielectric properties from ferroelectric (at $0 \leq x < 0.10$) to relaxor ferroelectric (at $0.10 \leq x \leq 0.25$), then to the properties, resembling those of dipolar glass with a weak or zero correlation between dipoles, even at low temperatures (at $0.25 < x \lesssim 0.90$), and then again to the relaxor ferroelectric properties (at $0.90 \lesssim x \leq 1$).

Acknowledgments

This work was supported by the Ministry of Science and Higher Education of Russia (project FSFZ-2022-0007), the equipment of the MIREA RTU Collective Use Center was used, which received the support of the Ministry of Education of the Russian Federation under the Agreement No. 075-15-2021-689 dated 01.09.2021.1.

ORCID

D. Yu. Fedulov  <https://orcid.org/0000-0003-4864-9784>
 K. E. Kamentsev  <https://orcid.org/0000-0002-1763-0012>
 A. A. Bush  <https://orcid.org/0000-0003-3990-9847>
 V. I. Kozlov  <https://orcid.org/0000-0003-2117-5056>

Appendix A

This section provides additional data on the temperature dependences of the permittivity and TSDC of the samples of the $(1-x)BT_xPFW$ system, which makes it possible to get a more complete picture of the evolution of the dielectric properties of the samples of this system when their composition changes.

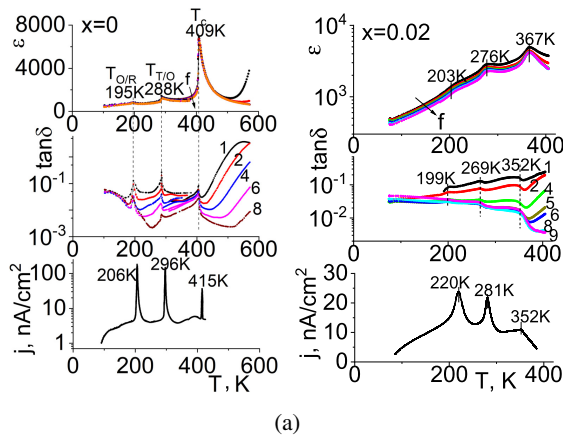


Fig. A.1. Dependences $\epsilon_1(T)$, $\tan\delta(T)$ (measured at f , kHz: 0.025 – curves 1, 0.120 – 2, 0.500 – 3, 1 – 4, 5 – 5, 10 – 6, 50 – 7, 100 – 8, 1000 – 9) and the density of TSDC for the $(1-x)BT_xPFW$ samples with $x = 0, 0.02, 0.05, 0.07, 0.10, 0.15, 0.25, 0.50, 0.60$ and 0.75 .

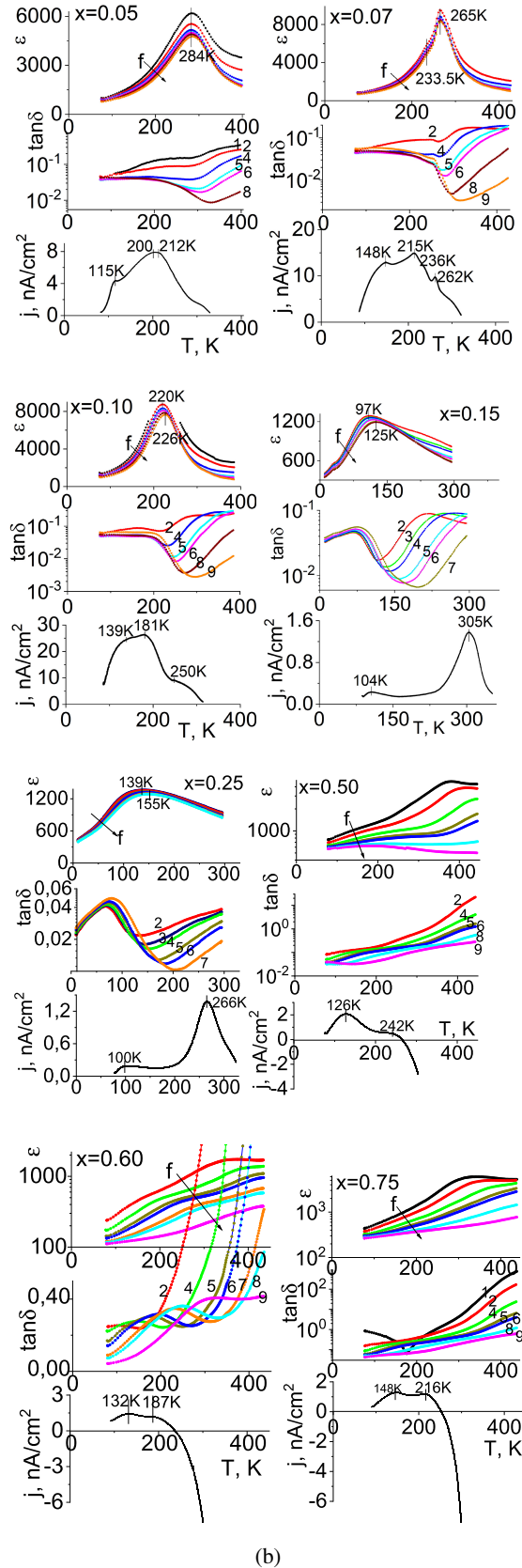


Fig. A.1. (Continued)

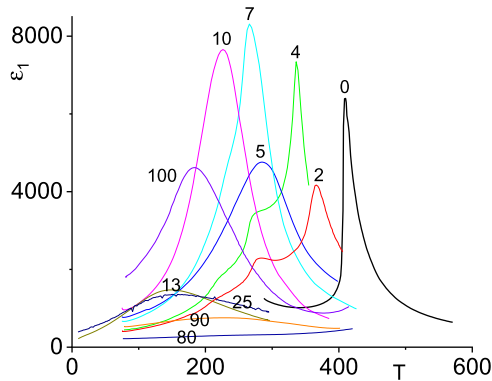


Fig. A.2. Dependences $\varepsilon_1(T)$ of the $(1-x)\text{BT} \cdot x\text{PFW}$ solid solutions, measured at $f = 1$ MHz (the numbers around the curves indicate $100x$).

References

- ¹B. Jaffe, W. R. Cook and H. Jaffe, *Piezoelectric Ceramics* (Academic Press, London, 1971).
- ²Yu. N. Venevtsev, E. D. Politova and S. A. Ivanov, *Segnetoelektriki i antisegetoelektriki semeistva titanata bariya (Ferro- and Antiferroelectrics of the Barium Titanate Family)*, Russian, (Khimiya, Moscow, 1985), p. 256 (in Russian).
- ³B. A. Rotenberg, *Keramicheskie kondensatornye dielektriki (Ceramic capacitor dielectrics)*, Russian, Tipografiya OAO NII "Girikond" (St. Petersburg, 2000), p. 246.
- ⁴M. Acosta, N. Novak, V. Rojas, S. Patel, R. Vaish, J. Koruza, G. A. Rossetti and J. Rödel, BaTiO₃-based piezoelectrics: Fundamentals, current status, and perspectives, *Appl. Phys. Rev.* **4**, 041305 (2017), doi: 10.1063/1.4990046.
- ⁵J. Gao, D. Xue, W. Liu, C. Zhou and X. Ren, Recent progress on BaTiO₃-based piezoelectric ceramics for actuator applications, *Actuators*, **6**, 24 (2017), doi: 10.3390/act6030024.
- ⁶Yu. N. Venevtsev, V. V. Sklyarevsky, I. I. Lukashevich, V. P. Romanov, N. M. Kotov, A. I. Kashulinsky, N. I. Filippov and A. S. Viskov, Investigation of the PbFe_{2/3}W_{1/3}O₃ – BaTiO₃ System, *Crystallography* **21**, 971 (1976).
- ⁷G. A. Smolenskii, A. I. Agranovskaya and V. A. Isupov, New ferroelectrics of complex composition Pb₂MgWO₆, Pb₃Fe₂WO₉, Pb₂FeTaO₆, *Sov. Phys. Solid State* **1**, 907 (1959).
- ⁸Yu. N. Venevtsev, V. V. Gagulin and V. N. Lyubimov, *Segnetomagnetiki (Magnetoelectric Materials)* (Nauka, Moscow, 1982), p. 224 (in Russian).
- ⁹Z.-G. Ye and H. Schmid, Electric Field induced effect on the optical, dielectric and ferroelectric properties of Pb(Fe_{2/3}W_{1/3})O₃ single crystals, *Ferroelectrics* **162**, 119 (1994), doi: 10.1080/00150199408245097.
- ¹⁰S. A. Ivanov, S.-G. Eriksson, R. Tellgren and H. Rundloof, Neutron powder diffraction study of the magnetoelectric relaxor Pb(Fe_{2/3}W_{1/3})O₃, *Mater. Res. Bull.* **39**, 2317 (2004), doi: 10.1016/j.materresbull.2004.07.025.
- ¹¹A. A. Bokov and Z.-G. Ye, Recent progress in relaxor ferroelectrics with perovskite structure, *J. Mater. Sci.* **41**, 31 (2006), doi: 10.1007/s10853-005-5915-7.
- ¹²D. Fedulov, V. Kozlov, A. Bush and M. Talanov, Preparation, X-ray phase analysis and dielectric properties of samples of the Pb(Fe_{1-x}Co_x)_{2/3}W_{1/3}O₃ and Pb(Co_{1-y}Fe_y)_{1/2}W_{1/2}O₃ ($0 \leq x, y \leq 1$) systems, *Ceram. Int.* **21**, 33219 (2022), doi: 10.1016/j.ceramint.2022.07.264.
- ¹³H. Takamizawa, K. Utsumi, M. Yonezawa and T. Ohno, Large capacitance multilayer ceramic capacitor, *IEEE Trans. Compon. Hybrids Manuf. Technol.* **V.CHMT-4**, 345 (1981), doi: 10.1109/TCHMT.1981.1135828.
- ¹⁴T. R. Shrout and A. Halliyal, Preparation of lead-based ferroelectric relaxors for capacitors, *Am. Ceram. Soc. Bull.* **66**, 704 (1987).
- ¹⁵Powder Diffraction files of the International Centre for Diffraction Data, PDF-2, Software version 4.19.21, database version 2.1901. <http://www.icdd.com/pdfse arch/>, 2019.
- ¹⁶R. D. Shannon, Revised effective ionic radii and systematic studies of interatomic distances in halides and chalcogenides, *Acta Crystallogr.* **32**, 751 (1976), doi: 10.1107/S0567739476001551.
- ¹⁷B. S. Kang, S. K. Choi and C. H. Park, Diffuse dielectric anomaly in perovskite-type ferroelectric oxides in the temperature range of 400–700°C, *J. Appl. Phys.* **94**, 1904 (2003), doi: 10.1063/1.1589595.
- ¹⁸X. Zhao, W. Qu, H. He, N. Vittayakorn and X. Tan, Influence of cation order on the electric field-induced phase transition in Pb(Mg_{1/3}Nb_{2/3})O₃-based relaxor ferroelectrics, *J. Am. Ceram. Soc.* **89**, 202 (2006), doi: 10.1111/j.1551-2916.2005.00675.x.
- ¹⁹T. Maiti, R. Guo and A. S. Bhalla, Structure-property phase diagram of BaZr_xTi_{1-x}O₃ system, *J. Am. Ceram. Soc.* **91**, 1769 (2008), doi: 10.1111/j.1551-2916.2008.02442.x.